Development of the Delamination Evaluation Parameters (I)
— The Delamination Aspect Ratio and the Delamination Shape Factors —

Cheol-Woong Kim*
Research Institute of Engineering & Technology, Korea University, 1, 5ga, Anam-dong, Sungbuk-gu, Seoul 136-701, Korea
Sam-Hong Song
Department of Mechanical Engineering, Korea University, 1, 5ga, Anam-dong, Sungbuk-gu, Seoul 136-701, Korea
Dong-Joon Oh
Department of Mechanical Education, Andong National University, 388, Songchun-dong, Andong, Kyoungbuk 760-749, Korea

Although the previous researches evaluated the fatigue behavior of Al/GFRP laminates using the traditional fracture mechanism, their researches were not sufficient to do it : the damage zone of Al/GFRP laminates was occurred at the delamination zone instead of the crack-metallic damages. Thus, previous researches were not applicable to the fatigue behavior of Al/GFRP laminates. The major purpose of this study was to evaluate delamination behavior using the relationship between crack length (a) and delamination width (b) in Al/GFRP laminate. The details of investigation were as follows : 1) Relationship between the crack length (a) and the delamination width (b), 2) Relationship between the delamination aspect ratio (b/a) and the delamination area rate ($(A_D)_N/(A_D)_{All}$), 3) The effect of delamination aspect ratio (b/a) on the delamination shape factor (f_S) and the delamination growth rate (dA_D/da). As results, it was known that the delamination aspect ratio (b/a) was decreased and the delamination area rate ($(A_D)_N/(A_D)_{All}$) was increased as the normalized crack size (a/W) was increased. And, the delamination shape factors (f_S) of the ellipse-II (f_{S3}) was greater than of the ellipse-I (f_{S2}) but that of the triangle (f_{S1}) was less than of the ellipse-I (f_{S2}).

Key Words : Delamination Width (b), Delamination Aspect Ratio (b/a), Delamination Shape Factor (f_S), Delamination Growth Rate (dA_D/da), Delamination Area Rate ($(A_D)_N/(A_D)_{All}$), Al/GFRP Laminates, Cyclic Bending Moment

1. Introduction

Hybrid composite materials such as Al/GFRP laminates show a superior fatigue behavior to general metallic materials (Guo and Wu, 1999 ; Jin and Mai, 1997 ; Yoon et al., 1995). In spite of it, the reason why the applicable fields were restricted is the delamination caused between the Al alloy layer and the fiber/epoxy one. This delamination greatly decreases the fiber bridging effect made between the Al alloy layer and the fiber/epoxy one. Therefore, the fatigue behavior of Al/GFRP laminates based on the delamination has been evaluated. The summary of them is as follows. 1) It was known that the delamination produced the semi-elliptic shape expanded to the back of cracks and that it was more affected by the loading direction than the loading type (Song and Kim, 2001). 2) Although the cracks under

* Corresponding Author,
E-mail : woong25@korea.ac.kr
TEL : +82-2-928-3608; **FAX** : +82-2-926-9290
Research Institute of Engineering & Technology, Korea University, 1, 5ga, Anam-dong, Sungbuk-gu, Seoul 136-701, Korea. (Manuscript **Received** February 20, 2004; **Revised** August 4, 2004)

the specific loading had to be observed in Al/GFRP laminates with a saw-cut, they could be made under the same condition in Al/GFRP laminates with a circular hole or not. However, the delamination should be made in any case. This reason was investigated through Average Stress Criterion (ASC) model and it was reported that the stacking sequence and the stress distribution at the vicinity of the notch were the major parameters to change the delamination shape (Song and Kim, 2003). 3) While the relationship between the crack length and the delamination area seemed regular, the relationship between the cycle and the delamination area was irregular. The delamination growth rate (dA_D/da) was also suggested to evaluate the delamination growth using the relationship between the crack length and the delamination area. In addition to the fiber bridging modification factor (β_{fb}), the fiber bridging effect factor (F_{BE}) to consider the delamination was suggested (Song and Kim, 2003). 4) In order to evaluate the expansion direction and the expansion rate of delamination, the delamination stress intensity factor range (ΔK_{Del}) was also suggested (Song and Kim, 2003). It was known that the coupling stiffness (B_{ij}) was increased and it made the growth of delamination faster when the stacking sequence was not symmetric. Through the above results, the delamination behavior of Al/GFRP laminates could be evaluated macroscopically. Summing up the above facts, the delamination was not determined just by the crack even though the first parameter to control the delamination was the crack length (a). The second parameter to control the delamination was the delamination width (b) as demonstrated in Fig. 1.

However, it is difficult to find the quantitative study of delamination using the relationship between the crack length and the delamination width. Therefore, the aim of this study is to evaluate the delamination behavior by relationship between the crack length and the delamination width. The details are as follows. First, the relationship between the crack length and the delamination width. Secondly, the relationship between the delamination aspect ratio (b/a) and the delamination area rate ($(A_D)_N/(A_D)_{All}$). Finally, the effect of the delamination aspect ratio on the delamination shape factor (f_S) and the delamination growth rate (dA_D/da). Through the above facts, the new parameters required for the delamination evaluation of the Al/GFRP laminates were proposed and the applied results were discussed.

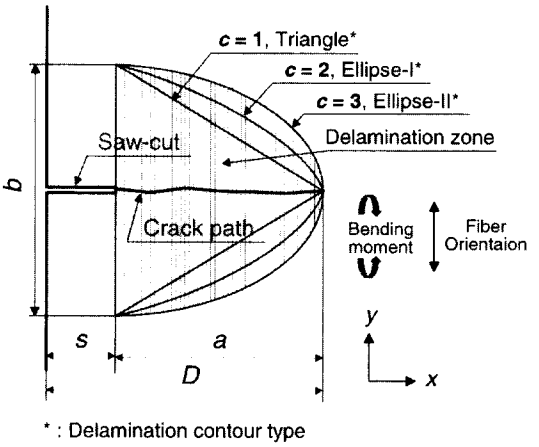

Fig. 1 The various delamination shapes and delamination elements in Al/GFRP laminates

2. Fabrication of Specimen and Experimental Method

2.1 Fabrication of Al/GFRP laminates specimen

The hybrid composites materials fabricated for this research was Al/GFRP laminates with the Al5052 alloy sheet and the unidirectional S-glass fiber/epoxy prepreg (volume fraction=45 %). Al/GFRP laminates were manufactured as the 2/1 type that the unidirectional S-glass fiber/epoxy was inserted between two Al5052 alloy sheets. At that time, the chromic acid anodizing was performed as the pre-procedure. The mechanical properties of the unidirectional S-glass fiber/epoxy prepreg and Al5052 alloy sheets were shown in Table 1 and 2.

The laminated specimens were cured by a hot-plate press. During the curing, the post-heating procedure was used to reflect the Differential Scanning Calorimetry (DSC) results of prepreg

Table 1 Mechanical properties of S-glass fiber

Fiber type	E_1 (GPa)	E_2 (GPa)	G_{12} (GPa)	ν_{12}	Ultimate tensile strength (MPa)	Tensile modulus (GPa)	Tensile strain to failure (%)	Density (g/cm^3)
S-glass	85.5	85.5	35.6	0.20	4600	86	5.3	2.55

Table 2 Mechanical properties of Al5052

Alloy	Tensile strength (MPa)	Yielding strength (0.2% offset) (MPa)	Thickness (mm)
Al5052	283	228	0.5

epoxy-resins and it made the specimens more stable chemically.

2.2 Configuration of Al/GFRP laminates specimen

The geometries of Al/GFRP laminates specimen were shown in Fig. 2. Pre-cracks were made at the low edge of the specimens by a wheel cutter and four holes (10.5 mm diameter) were drilled at the fixing area of specimens. The total thickness of the specimens was 2.1 mm since each thickness of S-glass fiber/epoxy prepreg and Al5052 alloy sheet was 0.5 mm.

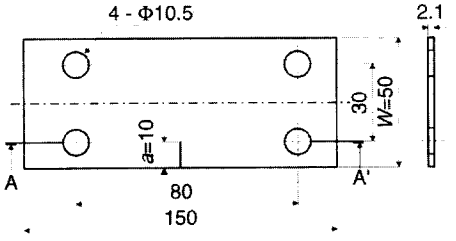

(a) Geometries of Al/GFRP laminate specimen

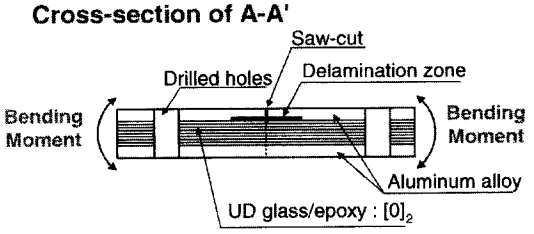

(b) Cross-section of Al/GFRP laminate specimen

Fig. 2 Geometries of specimen and cross-section view in Al/GFRP laminates

2.3 Fatigue test method by the cyclic bending moments

The fatigue tests were performed by the bending & torsion fatigue testing machine (TB-10, Shimadzu Co.) whose maximum moment was 98 N-m. The RPM and the frequency of this machine were 2,000 rpm and 33.3 Hz, respectively. While Al/GFRP laminates showed the very excellent fatigue characteristics under the tension-tension cyclic loading, the fatigue behavior under the tension-compression cyclic loading was definitely worse. It resulted from the weakness of GFRP (S-glass fiber/epoxy) layer under compression. Therefore, the stress ratio (R) of -1 was selected for this research to consider this characteristics sufficiently. The cyclic bending moment of 3.92 N-m was applied and the fatigue cracks were measured at 100 magnification by the travelling microscope. C-scan (Mi-SCOPE exla, Hitachi Co.) inspection was used to obtain the delamination images between the Al alloy sheet and S-glass fiber/epoxy one and those of corresponding cyclic delamination were recorded. Using these images, the length (a), the width (b), the contour (c) and the area (A_D) of delamination were obtained. To get the reliable results, ten specimens were tested and the average value of results was decided.

3. Experimental Results and Discussions

3.1 Relationship between the crack length (a) and the delamination width (b)

Unlike the monolithic metals, Al/GFRP laminates did not show the sudden change of the crack growth rate with increasing of cycles. During the second half of loading, this crack growth rate was the same as that of the first half of loading even though increasing of the crack length caused decreasing of ligament. Consequently, lin-

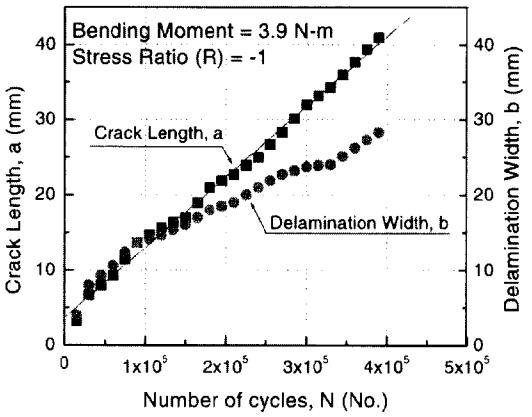

Fig. 3 Relationship between crack length (a) and cycles (N) vs. delamination width (b) and cycles (N) in Al/GFRP laminates

ear a-N relationship was obtained as Fig. 3. This phenomenon resulted from the stress bridging effect of fiber layer. However, if the crack propagated the delamination field between the Al5052 alloy layer and the S-glass fiber/epoxy one was initiated and grown.

The delamination was greatly affected by the crack rather than by the number of cycles (Song and Kim, 2003). It was possible to predict some special relationship between the crack and the delamination. When the major axes of delamination expansion direction were determined as x- and y- direction, it was known that the delamination length of x-axis direction was equal to the crack length. This fact made it possible to consider the crack length as the delamination length. In the meantime, the delamination width (b) corresponding to y-axis direction was broadened normal to the crack growth direction. From these facts, a lot of information about delamination behavior could be obtained using the relationship between the crack length (a) and the delamination width (b). For example, if the crack tip was connected to the edge of delamination width, the delamination contour length ($2c$) and the delamination area (A_D) could be calculated. Depending on the test condition, the delamination contour could become the various shapes as triangle ($c=1$), ellipse-I ($c=2$) and ellipse-II ($c=3$). In reality, the vague cases were made frequently such as the intermediate between the triangle and the ellipse. And so, the triangle model ($c=1$) was selected for this study. If the triangle model was applied, the contour length and the delamination area could be obtained easily by the crack length and the delamination width. Besides, since the direct measurement of the delamination width (b) was not possible, the calculation of the delamination width was carried out by the ultrasonic C-scan images. By the delamination images taken at each 1.5×10^4 cycles, the delamination width was converted to the real delamination width.

Figure 4 showed the delamination images taken at each 3.0×10^4 cycles and they were used to measure the basic elements of delamination such as the width (b), the contour length ($2c$) and the area (A_D) of delamination. The delamination behavior was simplified through the next assumptions. i) The crack and the delamination width should be linear. ii) The delamination type was the triangle. iii) The delamination was symmetric based on the crack. The relationship between the crack length (a) and the delamination width (b) in Fig. 3 and Fig. 4 was investigated under these assumptions. It was as follows. While the growth rate of crack showed linearity from the beginning to the end of cycle loading, the increase rate of delamination width became the lower along a quadric curve. Examining the increase of crack length and delamination width, crack length seemed to be equal to delamination width from the beginning to $N=1.5\times10^5$ cycles but crack length was greater than delamination width after $N=1.5\times10^5$ cycles. After the delamination width became about 18 mm, the growth rate of the delamination width was slow. This phenomenon could be observed by the delamination images in Fig. 4. The above region (a) ~ (e) of Fig. 4 showed $a=b$ and the middle one (f) ~ (k) meaned $a>b$. The bottom one (l) ~ (o) of Fig. 4 were the independent area where only the delamination grow after Al5052 alloy layer was fully fractured. If the crack growth was terminated due to the full-fracture of the Al5052 alloy layer, the type of delamination area gradually changed from the triangle to the square. At that time, the dela-

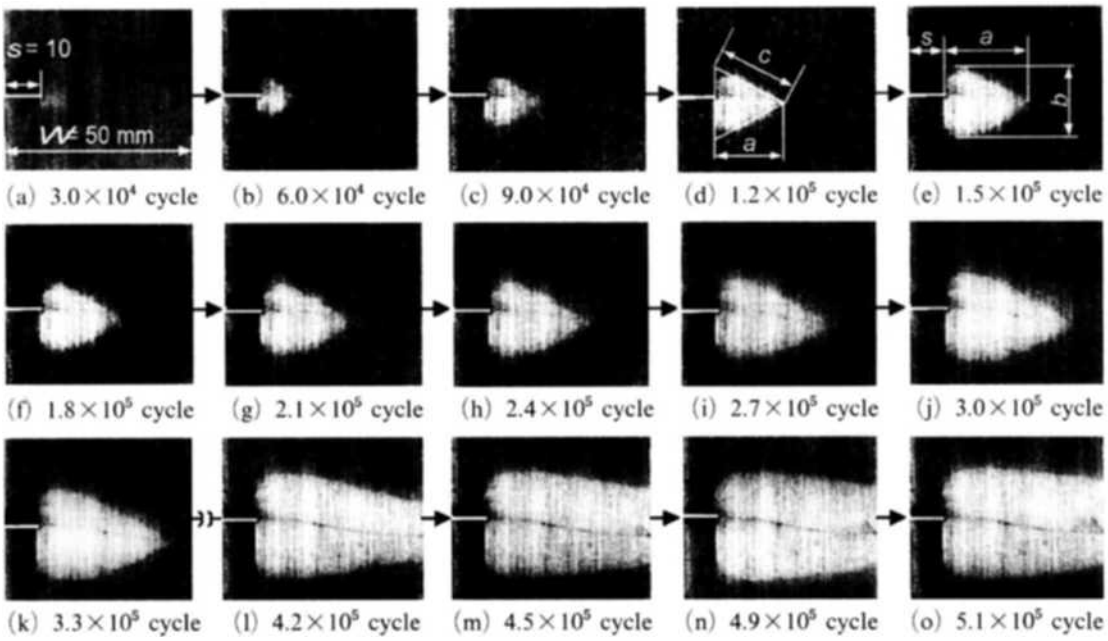

Fig. 4 Ultrasonic C-Scan images of the delamination elements (crack length (a), delamination width (b), delamination contoure (c)) in Al/GFRP laminates under cyclic bending moment

mination width was constant and the delamination contour (c) was expanded. Therefore, it was impossible to apply the delamination growth rate (dA_D/da) and the fiber bridging effect factor (F_{BE}) (Song and Kim, 2003) obtained by the relationship between the crack length and the delamination area after the end of crack growth. For this reason, the graphs in this chapter showed the behavior from the beginning to the end of the crack growth.

Fig. 5 was demonstrated to observe the relationship between the crack length and the delamination width definitely. After the crack length was equal to the delamination width for the initial crack length of 0 to 20 mm (a/W=0.2~0.6), the crack length was greater than the delamination width with increasing of the crack length. When the crack length was 20 to 30 mm (a/W=0.6~0.8), the delamination width approached about 80% of the crack length and it became about 70% of the crack length for 30 to 40 mm (a/W=0.8~1.0). Summing up, it was known that the growth rate of delamination width began to slow down from a/W=0.6 and it became greatly dull above a/W=0.8.

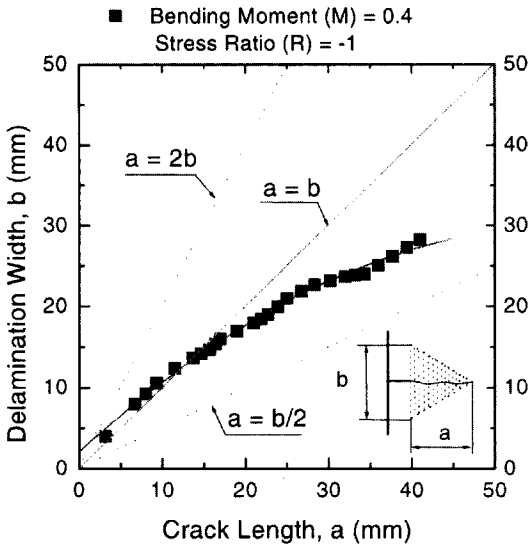

Fig. 5 Relationship between the delamination width (b) and the crack length (a) in Al/GFRP laminates

3.2 Relationship between the delamination aspect ratio (b/a) and the delamination area rate ($(A_D)_N/(A_D)_{All}$)

As mentioned at the previous section, it was

known that the growth rate of crack was constant but that of the delamination width was decreased with increasing of thd number of cycle (N) or the normalized crack size (a/W) by the examination of the relationship between the crack length (a) and the delamination width (b). Using the relationship between the crack length and the delamination width at this section, a new parameter such as the delamination aspect ratio (b/a) was suggested to obtain the delamination growth rate of the longitudinal direction (x-direction) and the longitudinal transverse direction (y-direction) in Fig. 1.

A new parameter such as the delamination area rate ($(A_D)_N/(A_D)_{All}$) was also proposed to calculate the growth rate of delamination area using an area rate (the total area ($(A_D)_{All}$) to be observed for the delamination versus the delamination area ($(A_D)_N$) at the specific cycle). The relationship between the delamination aspect ratio (b/a) and the normalized crack size (a/W) as well as the relationship between the delamination area rate ($(A_D)_N/(A_D)_{All}$) and the normalized crack size (a/W) was shown in Fig. 6. The delamination aspect ratio (b/a) was steadily decreased as the a/W was increased. The reason was that while the growth rate of crack was constant with increasing of the a/W. The growth rate of the delamination width was gradually decreased. On the other hand, the growth rate of delamination area rate ($(A_D)_N/(A_D)_{All}$) was slowly increased as the a/W was increased. While the a/W was increased, the growth rate of delamination width was decreased but that of crack length was constant. It resulted in the gradual increase of delamination area rate the ($(A_D)_N/(A_D)_{All}$). If the growth of delamination width was arithmetic, that of the delamination area (A_D) could be geometric. It was possible to observe the sudden increase of the delamination after the $a/W=0.8$. At first, it was guessed that the growth rate of crack would be faster due to the expansion of the damaged region if the delamination area rate ($(A_D)_N/(A_D)_{All}$) became increased. Consequently, the growth rate of crack was constant as shown in Fig. 3. In other words, it was clear that the magnitude of delamination

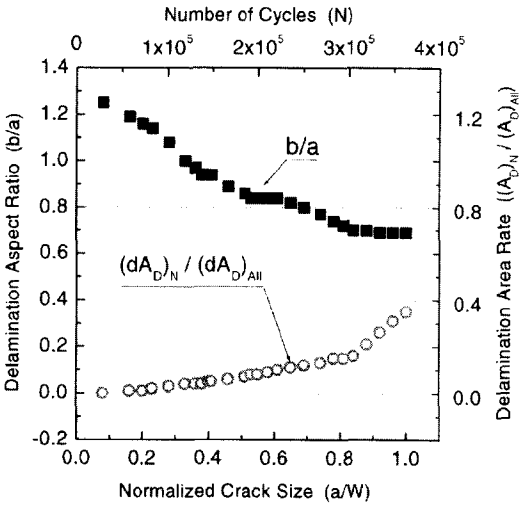

Fig. 6 Relationship between the delamination aspect ratio (b/a) and a/W vs. the delamination area rate ($(A_D)_N/(A_D)_{All}$) and a/W in Al/GFRP laminates

area did not affect the growth rate of crack.

3.3 The effect of delamination aspect ratio (b/a) on the delamination shape factor (f_S) and the delamination growth rate (dA_D/da)

It was shown that the delamination aspect ratio (b/a) was decreased as the normalized crack size (a/W) was increased at the previous section. It was believed that the change of the b/a could affect a major parameter to determine the delamination shape factor (f_S) and the delamination growth rate (dA_D/da). Considering the b/a as well as the f_S and dA_D/da proposed by Song and Kim (2003), it was discussed at this section whether any change could be made. It was confirmed that the delamination growth depended on the crack length rather than on the number of cycle from the previous researches. The equation to relate the area expansion rate of delamination to the increase of crack length was called the delamination growth rate and was written as Eq. (1).

$$\frac{dA_D}{da}=f_S\frac{(A_D)_n-(A_D)_{n-1}}{a_n-a_{n-1}} \tag{1}$$

Where, a was the crack length and A_D was the

delamination area. Since the cracked area was less than the A_D, it was neglected. The f_S was called the delamination shape factor. The f_S would be changed by the delamination type of the triangle ($c=1$), the ellipse-I ($c=2$) or the ellipse-II ($c=3$) like the c suggested in Fig. 1. Considering the b/a, f_S could be written as Eq. (2).

$$c=1,\ f_{S1}=\left(\frac{b}{a}\right)\left(1-\frac{s}{D}\right)$$
$$c=2,\ f_{S2}=\left(\frac{b}{a}\right)\sqrt{1-\left(\frac{s}{D}\right)} \qquad (2)$$
$$c=3,\ f_{S3}=\left(\frac{b}{a}\right)\sqrt{1-\left(\frac{s}{D}\right)^2}$$

Where, b, s and D were the delamination width, the saw-cut length and the sum of the saw-cut and the crack lengths, respectively. They were clearly demonstrated in Fig. 1. $c=1$, 2 and 3 represent the delamination shape of triangle, ellipse-I and ellipse-II, respectively.

Figure 7 showed the changing appearance of the f_S (f_{S1}, f_{S2}, f_{S3}) obtained from the above equations as the a/W was increased. The f_S of ellipse-II (f_{S3}) was greater than that of ellipse-I (f_{S2}) and that of triangle (f_{S1}) was the smallest in Fig. 7. While the f_{S3} was three times bigger than the f_{S1} at the beginning, the difference between the f_{S3} and f_{S1} was slowly decreased as the a/W was increased. Especially, the change of the f_{S1}, f_{S2}, f_{S3} was not observed from $a/W=0.8$ and their differences were also very small. Consequently, it was known that the effect of delamination shape on the delamination behavior was strong at the beginning but it was diminished as the crack grew. The effect of three different delamination shape factors (f_{S1}, f_{S2}, f_{S3}) on the behavior of delamination growth rate (dA_D/da) was considered in Fig. 8.

Figure 8 showed the behavior of the delamination growth rate according to the increase of cycles. There were two cases that three different type of the f_S (f_{S1}, f_{S2}, f_{S3}) were considered for the dA_D/da and were neglected. In general, the dA_D/da of the former was lower than that of the latter. Particularly, the dA_D/da of the f_{S1} became lower than those of the f_{S2} and f_{S3}. In other words, it was known that the dA_D/da of the triangle was distributed at lower part than those of the ellipses. For ellipses, it was clear that the dA_D/da of the f_{S2} was also lower than that of the f_{S3}. The averages of the f_{S1}, f_{S2} and f_{S3} obtained from Fig. 7 were $f_{S1}=0.57$, $f_{S2}=0.70$, $f_{S3}=0.87$. Comparing them with Fig. 8, they were as

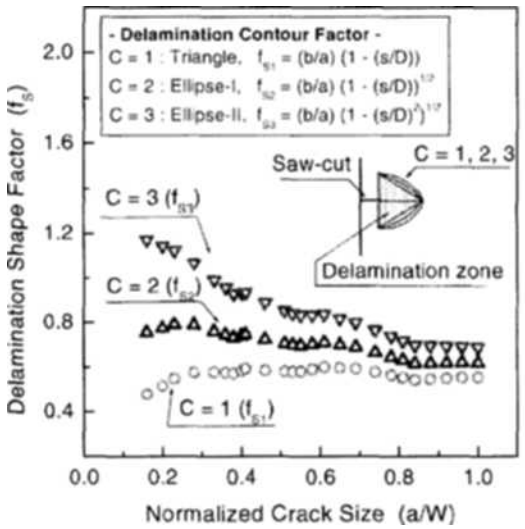

Fig. 7 Relationship between three different types of the delamination shape factors (f_{S1}, f_{S2}, f_{S3}) and the normalized crack size (a/W)

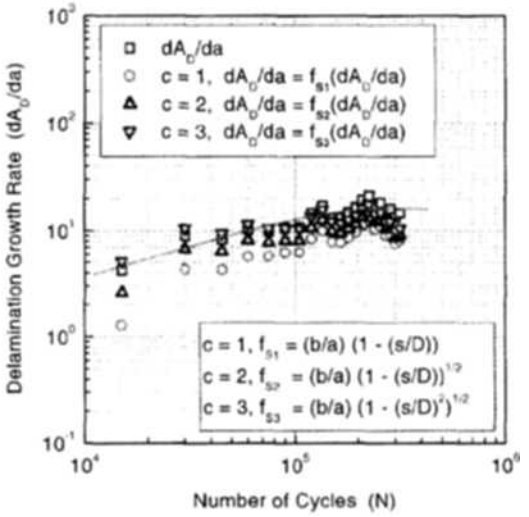

Fig. 8 Relationship between four different types of the delamination growth rate (dA_D/da) and the number of cycles (N)

follows. When the dA_D/da to consider the f_S compared with the dA_D/da to neglect the f_S, the latter was regarded as 100%. It was shown that the dA_D/da to consider the f_{S1}, f_{S2} and f_{S3}, were decreased about 43%, 30% and 13%, respectively. Therefore, among three different delamination growth rates (dA_D/da) to consider the f_S, the dA_D/da of the ellipse-II (f_{S3}) was the greatest but the dA_D/da of the triangle was the smallest. It was reported by Roebroeks (1987) that the fiber bridging effect of the triangular delamination was superior to that of the ellipse ones. For this reason, it was believed that the superiority of the fiber bridging effect made the delamination growth rate (dA_D/da) lower. It implied that the dA_D/da of the triangular delamination became lower than that of the elliptical ones. This result agreed well with the Roebroeks reports.

4. Conclusions

Using the relationship between the crack length (a) and the delamination width (b), the delamination behavior of Al/GFRP laminates was evaluated and the next conclusions were obtained.

(1) While the crack growth of Al/GFRP laminates showed linearity, the delamination width (b) growth rate was lowered along the quadric curve as the number of cycles were increased. Therefore, it was known that the relationship between the crack length (a) and the delamination width (b) remained $a=b$ at the beginning of cyclic loading but the crack length was greater than the delamination width after the middle of cycling.

(2) It was shown that the delamination aspect ratio (b/a) was slowly decreased and the delamination area rate $((A_D)_N/(A_D)_{All})$ was increased as the normalized crack size (a/W) was increased. However, the crack growth was nearly constant even though the delamination area rate was increased. Consequently, it was believed that the magnitude of delamination area was not the parameter to control the crack growth rate.

(3) The delamination shape factor (f_S) was changed by the delamination shape such as the triangle or the ellipse. The delamination shape factor of the ellipse-II (f_{S3}) was greater than that of the ellipse-I (f_{S2}) but that of the triangle (f_{S1}) was less than that of the ellipse-I (f_{S2}). While the differences among the f_{S1}, f_{S2} and f_{S3} seemed greater at the beginning of loading, these differences were decreased and became constant as the crack grew. Namely, the effect of the delamination shape on the delamination behavior was strong at the beginning of the cyclic loading but it was gradually diminished according to the increase of the a/W.

(4) Considering the effect of the delamination shape factor (f_{S1}, f_{S2}, f_{S3}) on the delamination growth rate (dA_D/da), it was clear that the delamination growth rate (dA_D/da) of the triangle was lower than that of the ellipse. This result was well coincident with the previous researches that the fiber bridging effect of the delamination triangular shape was superior to that of the elliptical ones.

Acknowledgment

This work was supported by grant No. R01-2003-000-10567-0 from the Korea Science & Engineering Foundation.

References

Guo, Y. J. and Wu, X. R., 1999, "Bridging Stress Distribution in Center-Cracked Fiber Reinforced Metal Laminates: Modeling and Experiment," *Engineering Fracture Mechanics*, Vol. 63, pp. 147~163.

Jin Zhi-He and Mai Yiu-Wing, 1997, "Residual Strength of an ARALL Laminate Containing a Crack," *Journal of Composite Materials*, Vol. 31, No. 8, pp. 746~761.

Roebroeks, G. H. J. J., 1987, "Constant Amplitude Fatigue of ARALL-2 Laminates," *Report LR-539*, Department of Aerospace Engineering, Delft University of Technology, Netherlands.

Song Sam-Hong and Kim Cheol-Woong, 2001, "The Delamination and Fatigue Crack Propagation Behavior in Al5052/AFRP Laminates Under Cyclic Bending Moment," *Transaction of the*

KSME, A, Vol. 25, No. 8, pp. 1277~1286.

Song Sam-Hong and Kim Cheol-Woong, 2003, "Fatigue Crack and Delamination Behavior in the Composite Material Containing a Saw-cut and Circular Hole (I)—Aramid Fiber Reinforced Metal Laminates-," *Transactions of the KSME, A*, Vol. 27, No. 1, pp. 58~65.

Song Sam-Hong and Kim Cheol-Woong, 2003, "The Analysis of Fatigue Behavior Using the Delamination Growth Rate (dA_D/da) and Fiber Bridging Effect Factor (F_{BE}) in Al/GFRP Laminates," *Transactions of the KSME, A*, Vol. 27, No. 2, pp. 317~326.

Song Sam-Hong and Kim Cheol-Woong, 2003, "Analysis of Delamination Behavior on the Stacking Sequence of Prosthetic Foot Keel in Glass Fiber Reinforced Laminates," *Transactions of the KSME, A*, Vol. 27, No. 4, pp. 623~631.

Yoon, H. K., Cheng, H. Y., Park, W. J. and Hue, C. W., 1995, "The Behavior of Crack Growth Rate for APAL and CPAL Patched with FRP Laminate in Aluminum Alloy Plate," *Transactions of the KSME, A*, Vol. 19, No. 4, pp. 253~262.